Numerical simulation of PCBM and MoO_3 stacked electron and hole transport layer based perovskite solar cell

A PROJECT REPORT

SUBMITTED IN PARTIAL FULFILLMENT OF
THE REQUIREMENTS FOR THE AWARD OF
DEGREE
OF

MASTERS OF TECHNOLOGY
IN
NANOSCIENCE AND TECHNOLOGY

Submitted By:

Nishant Singhal **2K16/NST/05**

Under the supervision of

Dr. Rishu Chaujar
Assistant Professor
DEPARTMENT OF APPLIED PHYSICS

DEPARTMENT OF APPLIED PHYSICS
DELHI TECHNOLOGICAL UNIVERSITY, DELHI
(Formerly Delhi College of Engineering)
Bawana Road, Delhi-110042 July, 2018

DEPARTMENT OF APPLIED PHYSICS

DELHI TECHNOLOGICAL UNIVERSITY, DELHI
(Formerly Delhi College of Engineering)
Bawana Road, Delhi-110042

CANDIDATE'S DECLARATION

I, NISHANT SINGHAL, Roll No. 2K16/NST/05, student of M. Tech. Applied Physics, hereby declare that the project Dissertation titled "**Numerical simulation of PCBM and MoO_3 stacked electron and hole transport layer based perovskite solar cell"** which is submitted by me to the Department of APPLIED PHYSICS, Delhi Technological University, Delhi in the partial fulfillment of the requirement for the award of the degree of Master of Technology, is original and not copied from any source without proper citation. This work has not previously formed the basis for the award of any Degree, Diploma Associate ship, Fellowship or other similar title or recognition.

Place: New Delhi **Nishant Singhal**

Date: **2K16/NST/05**

DEPARTMENT OF APPLIED PHYSICS
DELHI TECHNOLOGICAL UNIVERSITY, DELHI
(Formerly Delhi College of Engineering)
Bawana Road, Delhi-110042

CERTIFICATE

I hereby certify that the Project Dissertation titled "**Numerical simulation of PCBM and MoO_3 stacked electron and hole transport layer based perovskite solar cell"** which is submitted by Nishant Singhal, Roll No. 2K16/NST/05 of Delhi Technological University, Delhi in partial fulfilment of the requirement for the award of the degree of Master of Technology, is a record of the project work carried out by the students under my supervision. To the best of my knowledge this work has not been submitted in part or full for any Degree or Diploma to this University or elsewhere.

Place: New Delhi **Dr. RISHU CHAUJAR**

Date: SUPERVISOR

Assistant Professor

Department of Applied Physics

Delhi Technological University

ACKNOWLEDGEMENT

During the time of my project, several people support my work and I would like to take this opportunity to acknowledge them.

First and foremost, I would like to express my sincere gratitude to my supervisor, mentor Dr. Rishu Chaujar, for her constant encouragement, support and guidance at every stage of my research period. She provided me every opportunity to present my work. I especially thank her for prompt reading and careful review of my thesis.

I am thankful to Delhi Technological University for generous support and providing ample infrastructure to carry out my research work.

ABSTRACT

In this study, a perovskite based solar cell device has been proposed and the power conversion efficiency, fill factor, open circuit voltage and short circuit current density of the proposed device was analyzed. When simulated, it achieves a power conversion efficiency of over 14% with AM 1.5 illumination. This type of perovskite solar cell has shown potential towards achieving a low cost and efficient solar energy conversion method and unlike its silicon counterparts, it has none of the disadvantages that are present in silicon based solar cells.

Different materials and their combinations were used as electron transport layer and hole transport layer. Materials that were used as electron transport layer resulted in short circuit current density of 17.92 $mA.cm^{-2}$. When a combination of two materials were used as hole transport layer, it has been observed that the external quantum efficiency is close to 55% in the 350-450 nm range which corresponds to high power conversion efficiency of 14.27% but the open circuit voltage showed little variation around 1.02 volts .

When MoO_3 is used as a hole transport layer and its thickness and doping was optimized, it was observed that there is a 60% increase in the short circuit current density as the thickness of MoO_3 was decreased and a 2% decrease in the PCE and FF with increase in thickness. When the doping of MoO_3 is varied, the external quantum efficiency went down from 55% to 50%.

Detailed realistic technology computer aided design (TCAD) analysis has been performed to predict the behavior of the device.

CONTENTS

LIST OF FIGURES

CHAPTER 1

INTRODUCTION

1.1 Renewable Energy Sources

There is a grave energy crisis across the world and the need for renewable energy sources is increasing. Not only these sources are available in abundance but they are also pollution free. Energy from the radiation of sun commonly known as solar energy is one such source, it is available in abundance and is pollution free. Earlier the equipment and machinery required for converting solar energy into electrical energy was expensive but in the 21st century with the advancement in research, the cost of equipment has considerably come down. Although there are many renewable energy sources available like wind energy, tidal energy, hydro power energy etc, the solar energy is most sought after source due to its easy availability and abundance.

1.2 Solar Cell

1.2.1 Solar PV effect

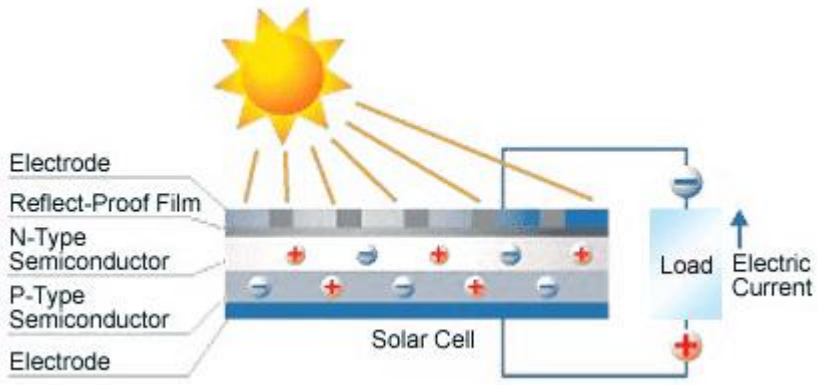

Figure 1.1: Working of a Solar Cell

The collection of light-generated carriers does not by itself give rise to power generation. In order to generate power, a voltage must be generated as well as a current. Voltage is generated in a solar cell by a process known as the "photovoltaic effect". The collection of light-generated carriers by the *p*-*n* junction causes a movement of electrons to the *n*-type

side and holes to the *p*-type side of the junction. Under short circuit conditions, there is no build up of charge, as the carriers exit the device as light-generated current.

However, if the light-generated carriers are prevented from leaving the solar cell, then the collection of light-generated carriers causes an increase in the number of electrons on the *n*-type side of the *p*-*n* junction and a similar increase in holes in the *p*-type material. This separation of charge creates an electric field at the junction which is in opposition to that already existing at the junction, thereby reducing the net electric field. Since the electric field represents a barrier to the flow of the forward bias diffusion current, the reduction of the electric field increases the diffusion current. A new equilibrium is reached in which a voltage exists across the *p*-*n* junction. The current from the solar cell is the difference between I_L and the forward bias current. Under open circuit conditions, the forward bias of the junction increases to a point where the light-generated current is exactly balanced by the forward bias diffusion current, and the net current is zero. The voltage required to cause these two currents to balance is called the "open-circuit voltage". The solar cell device is therefore also called as Photovoltaic (PV) device as it is based on the PV effect.

1.2.2 Diode Equation

Solar cell is a p-n junction diode that transforms solar energy into electrical energy

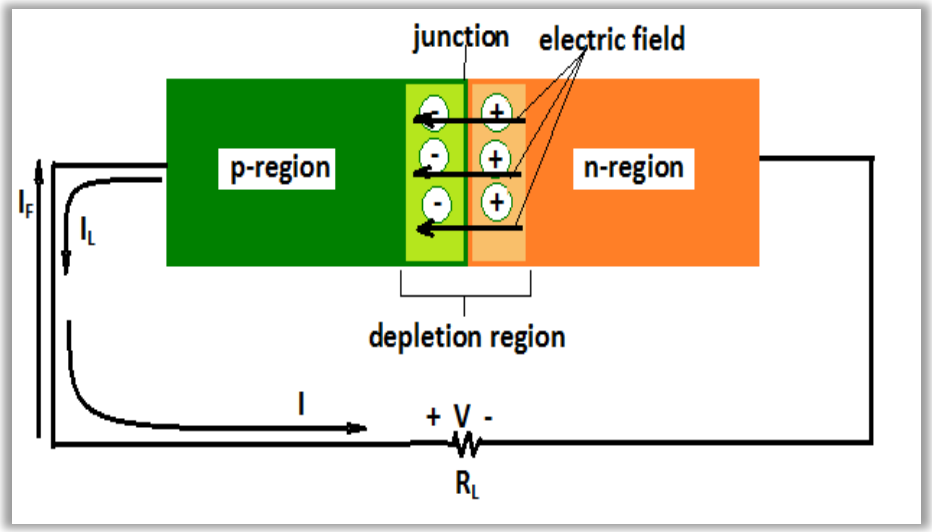

Figure1.2: Direction of light generated current in solar cell

$$I = I_L - I_F \text{..... eq. (1)}$$

$$I = I_L - I_S \left[exp\left(\frac{qV}{K_B T}\right) - 1\right] \text{..... eq. (2)}$$

Where I_L is light generated current

I_F is forward diffusion current,

I_S is saturation current,

q is charge of electron (1.6×10^{-19} C),

V is voltage generated,

K_B is Boltzmann Constant (1.38×10^{-23} J/K),

T is temperature

1.3 Parameters of Solar cell

There are few parameters with which the performance of a solar cell is analysed. They are listed below

1.3.1 Power Conversion Efficiency (PCE)

PCE is the ratio of output electrical power to input optical power

$$\eta = \left(\frac{V_{OC} I_{SC} FF}{P_{in}}\right) * 100\ \% \text{ ..... eq. (3)}$$

1.3.2 Fill Factor (FF)

It is a measure of realizable power from solar cell

$$FF = \frac{V_m I_m}{V_{OC} I_{SC}} \text{ ..... eq. (4)}$$

V_m is the max voltage generated and I_m is the max current flowing through the device

1.3.3 Open Circuit Voltage

It is the voltage obtained when the current is zero

$$V_{OC} = \frac{nkT}{q} \ln\left(\frac{I_L}{I_0} + 1\right)$$ ..... eq. (5)

where I_o is the saturation current and

n is the ideality factor

$$V_{oc} = \frac{kT}{q} \ln\left[\frac{(N_A + \Delta n)\Delta n}{n_i^2}\right]$$ ..... eq. (6)

N_A is the doping concentration,

Δn is the excess carrier concentration and

n_i is the intrinsic carrier concentration

1.3.4 Short Circuit Current Density

It is the current density when the voltage is zero which is equal to the light generated current density

$$Jsc = \left(\frac{I_{SC}}{area\ of\ active\ layer}\right) = \left(\frac{I_L}{areaof\ active\ layer}\right)$$ ..... eq. (7)

1.3.5 External Quantum Efficiency

It is the ratio of number of electron hole pairs collected by the solar cell to the ratio of number of photons incident on the solar cell. It considers the effect of optical losses like transmission and reflection.

1.4 Recombinations in Solar cell

- Radiative Recombination or Band to Band Recombination

  In this, there is a direct recombination between electron from conduction band with a hole from valence band. This phenomenon more readily takes place in direct

bandgap semiconductors such as GaAs. The photon emitted as a result has an energy signature similar to the bandgap but it is only weakly absorbed.

- Shockley Read Hall (SRH) Recombination

  This type of recombination takes place through defect levels. There are defects in the crystal lattice which introduces forbidden regions, the energy state of these forbidden regions traps an electron or a hole. If a hole or electron moves up to the same energy state before being thermally re emitted into the conduction band then it recombines with the electron or hole trapped there.

- Auger Recombination

  It takes place involving 3 carriers, an electron or a hole recombine but rather than emitting energy as heat or as photon the energy is gitven to a third carrier, an electron in the conduction band. The third excited electron then thermalizes back to the conduction band edge and recombines with a hole.

  The Radiative Recombination is a direct recombination whereas the other two are indirect recombinations. The radiative recombination takes place at a faster rate in low bandgap and weakly doped materials but as the bandgap and doping is increased the auger recombination becomes more dominant.

1.5 Need for evolution of materials used in solar cell

There is a monopoly of crystalline silicon (c-Si) solar cells in the global photovoltaic (PV) market for some decades now, capturing a market share of about 90%[1]. During the last 15 years only a marginal improvement in the efficiency of c-Si has been observed; 26.3% was the highest wafer size efficiency obtained so far with amorphous silicon (a-Si)/c-Si heterojunction technology[2] which has come quite close to the 29.4% theoretical maximum efficiency mark[3,4]. Even with all of this, a cheaper and economically feasible energy efficient module is needed so that the PV system market becomes competitive with the conventional energy market. In order to achieve efficiency higher than the practical and theoretical limit or to achieve ultrahigh conversion efficiency, a different structure with a different absorbent material with a tunable wide bandgap is needed. The solar cell with a different material and an analogous structure has been forecasted. But even with all of this the inherent need to do away with the silicon based solar cells, needs to be understood. This

point can be substantiated by running through the drawbacks of silicon which are listed below

- It has an indirect optical band gap that requires a thick active layer for the solar conversion and thus costly fabrication of large area materials.
- Efficiency losses for energy conversion, such as “red losses” at high wavelengths below the bandgap and “blue losses” at low wavelengths above the bandgap of silicon.
- In indirect bandgap semiconductors, change in energy (due to photon) and change in momentum (due to phonon) is required for movement of charge carrier form valence band to conduction band but in direct bandgap semiconductors, only a change in energy (due to photon) in required.
- Low absorption of silicon implies more thickness of active silicon layer in PV cell.

1.6 Perovskite

A mineral discovered by Gustav Rose in the Ural Mountains located in Russia. It is named in the memory of a Russian mineralogist Lev Perovski. Perovskite's crystal structure, its physical and chemical properties were first explained in 1926 by German Physicist Victor Goldschmidt, by the way of tolerance factors[5].

1.6.1 Structure of Perovskite

Perovskites, with a formulae of ABO_3 generally exists with a cubic structure and they crystallize in the orthorhombic. An A-site ion which is usually an alkaline earth element is present on the corners of the lattice, at the central position of the lattice B-site ions are present which are most likely to be 3d, 4d, and 5d metal or transition metal elements. For stability, if the tolerance factor t is in the range of 0.75–1.0[5], then the structure is considered stable. Most of the metallic elements are stable in the perovskite structure.

$$t = \frac{R_A + R_O}{\sqrt{2}\,(R_B + R_O)} \text{.....eq. (8)}$$

where *t* is the tolerance factor, R_A, R_B and R_O are the ionic radii of *A* and *B* site elements and oxygen respectively.

1.6.2 Physical Properties of Perovskite

- Lustre: They have a varying lustre from sub metallic to metallic, colorless streak, accompanied by imperfect cleavage and tenacity is oddly brittle.
- Color: They are found in various colors like black, brown, and gray, orange to yellow.

Perovskite crystals are often mistaken for galena but unlike perovskite galena has a better metallic luster, greater density, perfect cleavage and true cubic symmetry.

Organo metal halides based solar cells are at the forefront of the PV technology. Of late, the perovskite solar cells have become attractive candidates for solar cell structures due to their high efficiency. Suitable tunable bandgap of (1.55-2.3 eV) depending on the halide content, sharp absorption edge accompanied by little sub bandgap absorption[6], and high absorption coefficient[7] are the appealing properties of the methylammonium–lead–-halide, $CH_3NH_3PbX_3$ (X ¼ Br, I). In addition to all this, an unconventional boost in PCE over the last few years has made perovskite solar cells a strong contender for the next generation of PV technology[8].

Lately, two lead halide perovskite material which are similar in properties but differ in their chemical composition have come up as very strong contenders as absorbent materials in the solar cell, they are $CH_3NH_3PbI_3$ and $CH_3NH_3Pb_{3-x}Cl_x$. Although their charge generation and charge transport properties are yet to be fully understood, their two properties[6-8, 12] stand out

- Their charge diffusion length is greater than the absorption depth.
- It enables high efficiency photon harvesting and minimises charge collection losses.

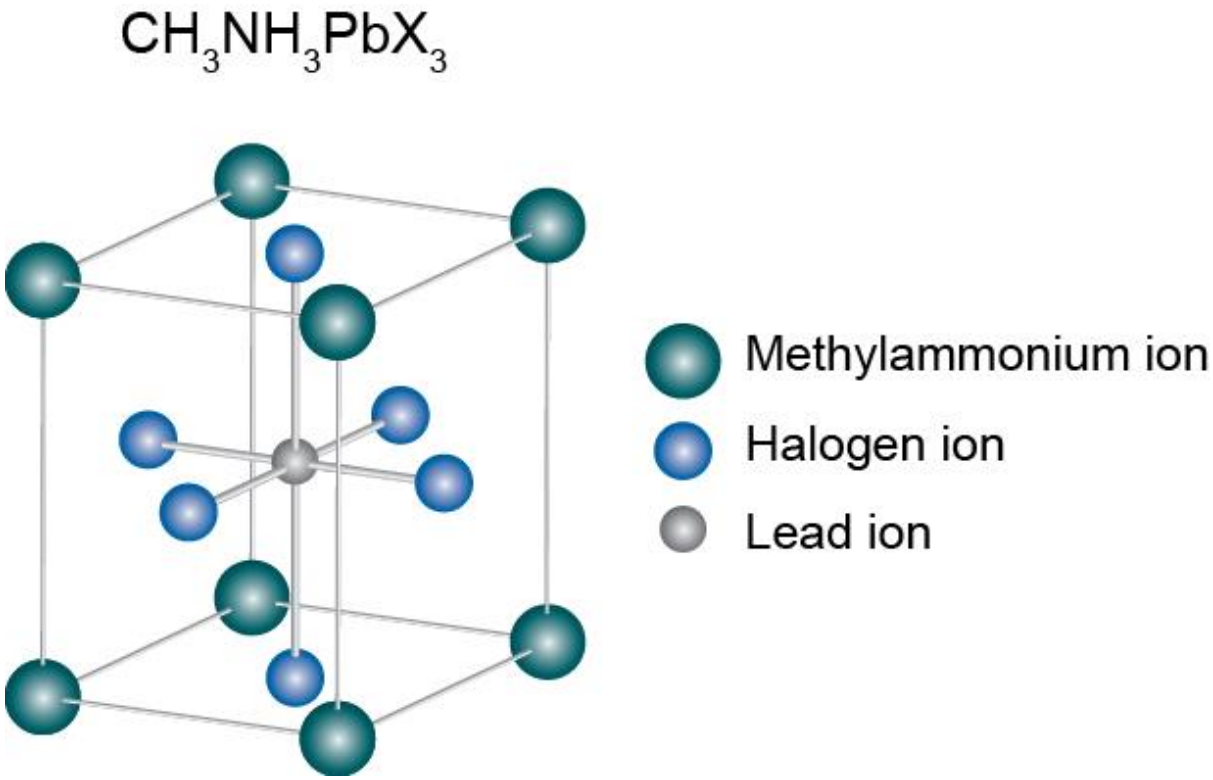

Figure 1.3: Structure of methyl ammonium lead halide perovskite material

1.7 Hole transport Layer and Electron Transport Layer

In the perovskite based PV cells, hole transport layer (HTL) and electron transport layer (ETL) are used to minimize recombination of the electron hole pair generated in the perovskite layer so as to maximize the power conversion efficiency[10]. This takes place chiefly because of two reasons:-

- If an HTL or ETL is present, then the electrons or holes cannot flow directly to the anode or cathode so by incorporating ETL and HTL the leakage current can be reduced, this is illustrated by the fact that the devices without ETL and HTL have high shunt resistances in comparison to the devices with ETL and HTL.
- The ETL and HTL have faster charge transport properties as compared to the active layer which is perovskite in this case. It means that they offer low resistance to the path of the charge carrier so the charges that reach the interface of ETL/HTL and

then can quickly move away from the active (absorbent) material which helps in minimising or controlling charge recombination taking place in the active layer.

1.7.1 ETL and its characteristics

The ETL, also known as the electron extraction layer or electron collection layer is basically a n type semiconductor; the layer into which the electrons are injected from the absorber perovskite layer, the electrons are then transported through the electron transporting materials (ETM), and then ultimately collected by the cathode.

One of the most significant features of an ETL is that it should be band aligned with the perovskite layer which means that the lowest unoccupied molecular orbital (LUMO) and highest occupied molecular orbital (HOMO) should be higher than the perovskite active layer[10, 16]. The second criterion is that it should have high transmittance in the UV-V region of the spectrum so that a photon can easily travel through it and be absorbed by the perovskite absorber[10, 11]. The final characteristic of the ETL is that the exciton generated via light absorption, moving across the perovskite layer, must be dissociated before being collected by the ETL[11].

In this work, compact TiO_2 and PCBM have been used as ETL. All the parameters used in the simulation along with the electrical and optical properties for the ETL materials used have been listed below

1.7.2 HTL and its characteristics

The HTL is basically the counterpart of ETL and is used to transport holes instead of electrons; a p type semiconductor device in which the holes are injected from the absorber perovskite layer, these holes travel through the Hole Transport Material (HTM) and finally collected by the anode.

The most important criterion that a HTL must fulfil is the band alignment with the perovskite layer which means that the lowest unoccupied molecular orbital (LUMO) and highest occupied molecular orbital (HOMO) should be lower than the perovskite active layer[10]. The next condition is that it should have high transmittance in the IR region of the spectrum so that a photon can easily travel through it and be absorbed by the perovskite

absorber[11]. The final characteristic of the HTL is that the exciton generated via light absorption, moving across the perovskite layer, must be dissociated before being collected by the HTL at its interface[11].

In this work, compact Spiro OMeOTAD and Molybdenum Trioxide (MoO_3/Moly) have been used as HTL. All the parameters used in the simulation along with the electrical and optical properties for the ETL materials used have been listed below

ETL/HTL which have inorganic material as their constituents has a longer electron/hole diffusion length as opposed to ETL/HTL made out of organic and ploymer materials[11].

The different properties listed for the perovskite makes it a prime candidate for the primary absorption layer in the solar cell architecture[9, 16, 17, 20]. Different semiconductor materials such as Spiro MeOTAD and molybdenum trioxide as HTL and Compact TiO_2 and PCBM as ETL[7,19] and a combination of these have been used in this work and their comparative study in terms of PCE, fill factor (FF), open circuit voltage(Voc) and short circuit current density (Jsc) has been done. The external quantum efficiency (EQE) and short circuit current density and voltage (J-V) characteristics have been compared to draw out the best material or a combination of materials. The simulations performed are under AM 1.5 illumination. All the structures proposed are two terminal devices simulated in TCAD silvaco atlas software.

Parameter	**Compact TiO_2**	**Perovskite**	**Spiro OMeOTAD**	**PCBM**	**MoO_3**
Mobility (cm^2/Vs)	0.006	50	0.0001	0.001	0.72
Bandgap (eV)	3.2	1.5	2.91	1.1	3.1
Conduction band density (cm^{-3})	10^{21}	$2.5x10^{20}$	$2.5x10^{20}$	10^{21}	$2.5x10^{20}$
Valence band density (cm^{-3})	$2x10^{22}$	$2.5x10^{20}$	$2.5x10^{20}$	$2x10^{22}$	$2.5x10^{20}$
Affinity (eV)	4	3.93	2.2	4.3	6.7
Permittivity	100	30	3	3.8	5.31
Carrier lifetime (sec)	10^{-7}	10^{-6}	10^{-9}	10^{-12}	10^{-9}

Table showing the optical and electronic parameters used in simulation

The parameters listed above for perovskite, spiro and tio_2 are as reported by Pandey *et al* [13] the parameters. The parameters listed above for the MoO_3 and PCBM material are taken from the literature [10, 14-17, 19]

The SRH, Radiative and Auger recombination rate for the perovskite material used are 10^{-5} cm^{-3}/s, $1.5x10^{-10}$ cm^{-3}/s and $3.4x10^{-28}$ cm^{-3}/s respectively[13].

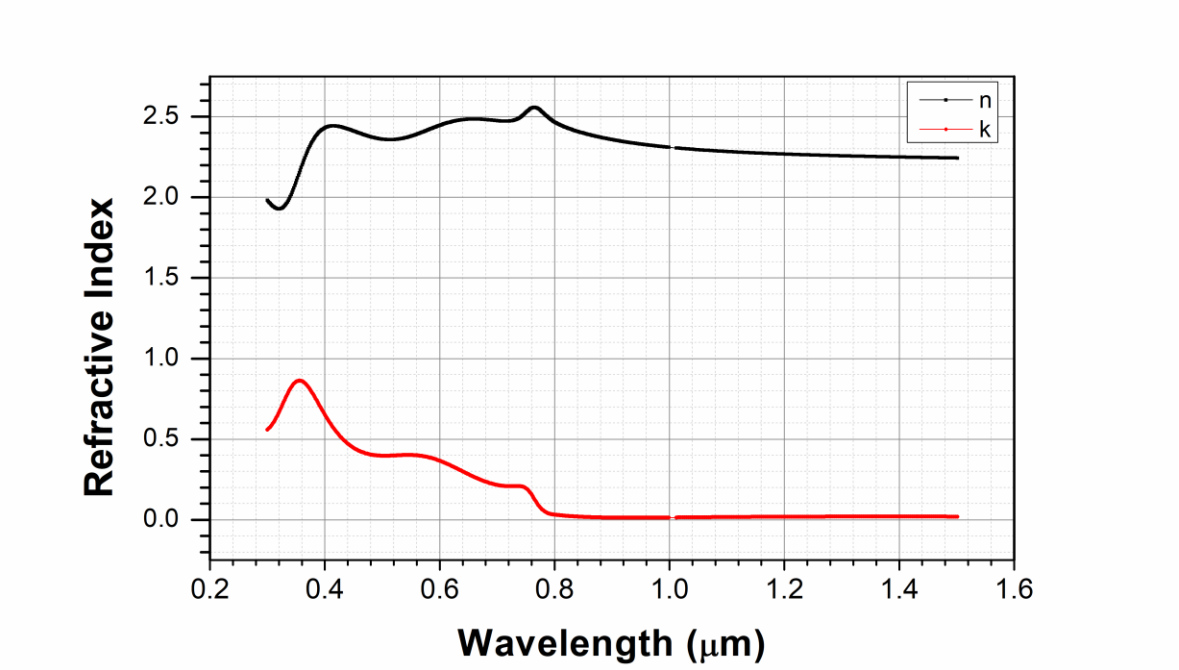

(a)

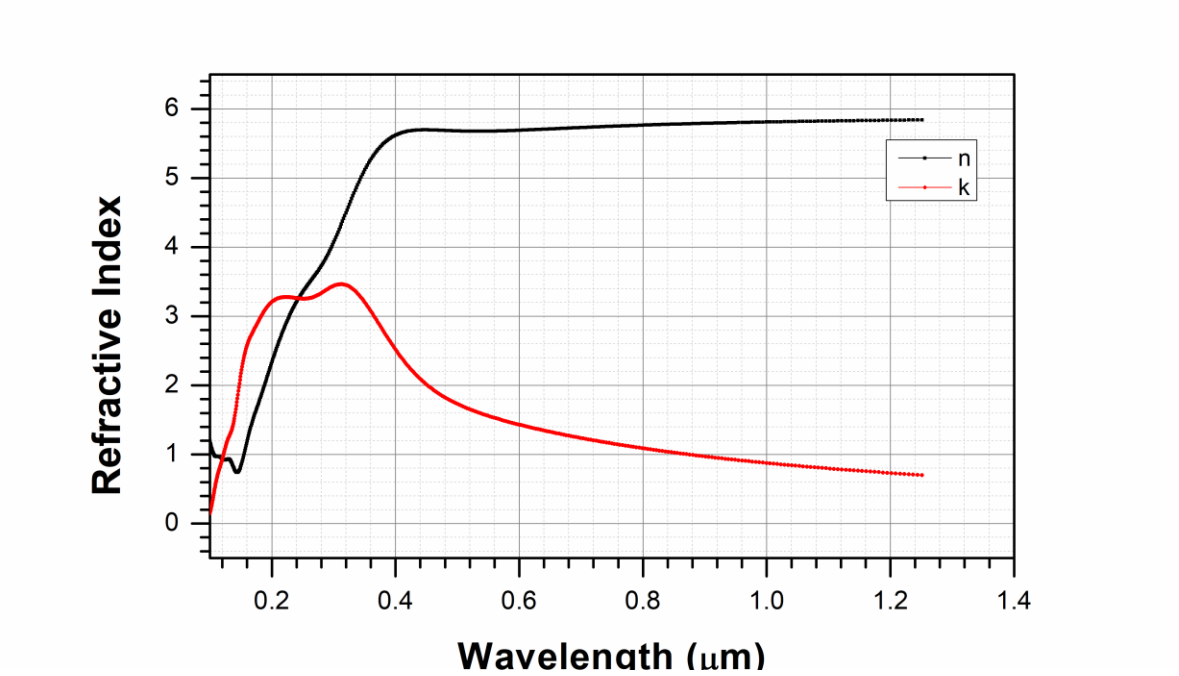

(b)

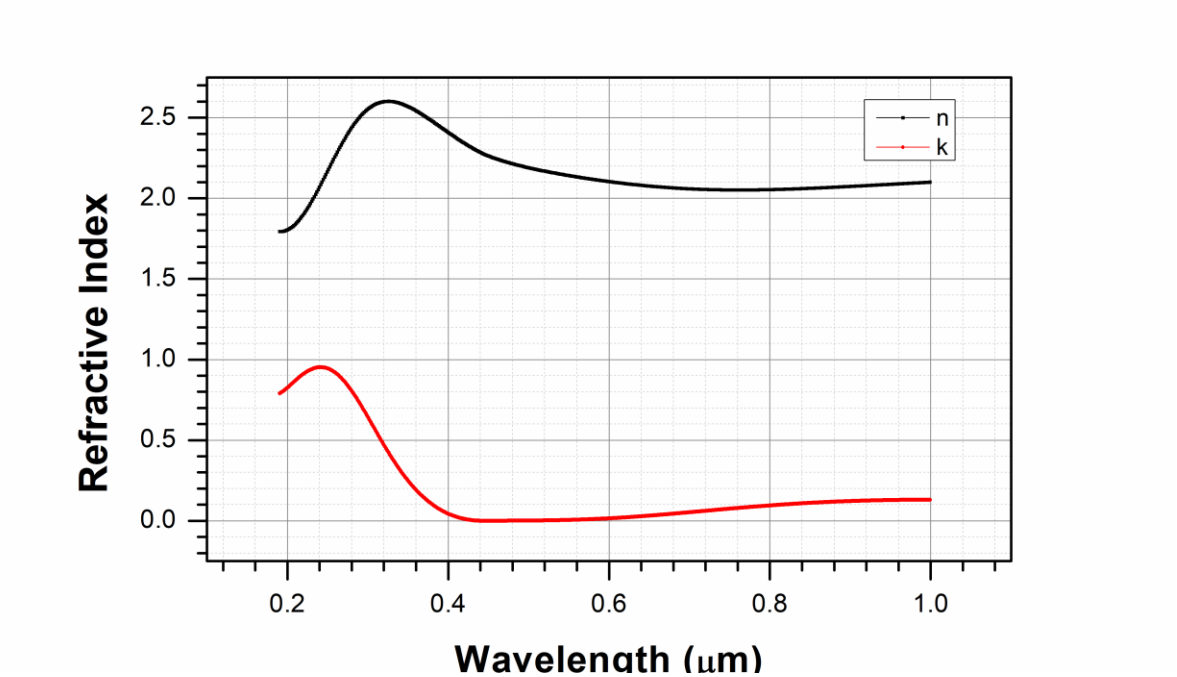
Refractive Index
Wavelength (μm)
n
k
2.5
2.0
1.5
1.0
0.5
0.0
0.2
0.4
0.6
0.8
1.0

(c)

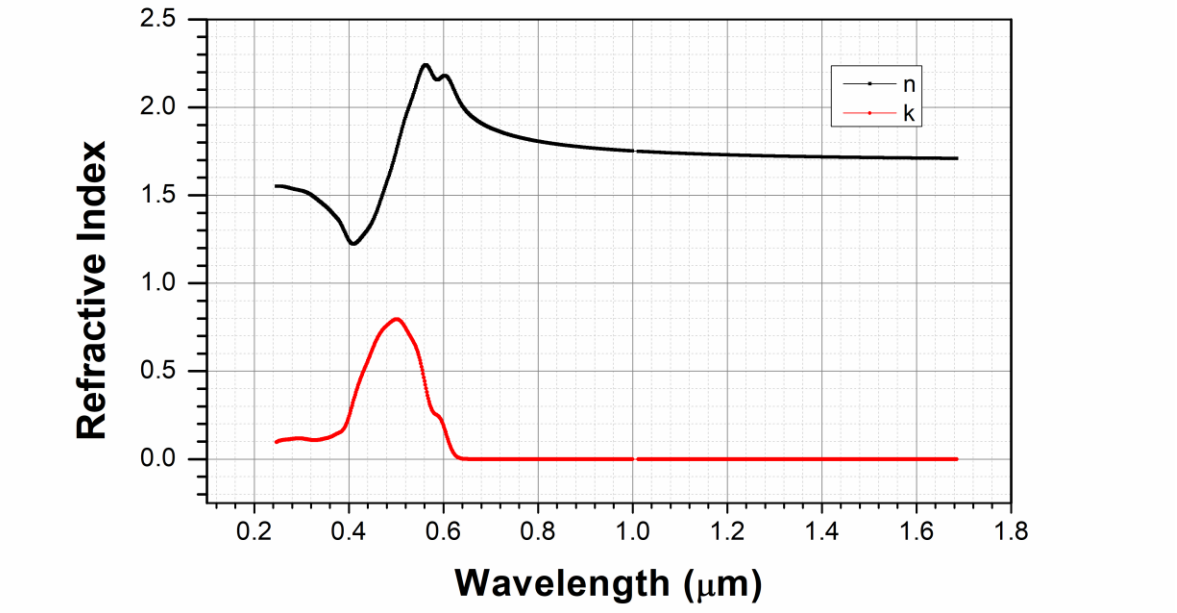
Refractive Index
Wavelength (μm)
n
k
2.5
2.0
1.5
1.0
0.5
0.0
0.2
0.4
0.6
0.8
1.0
1.2
1.4
1.6
1.8

(d)

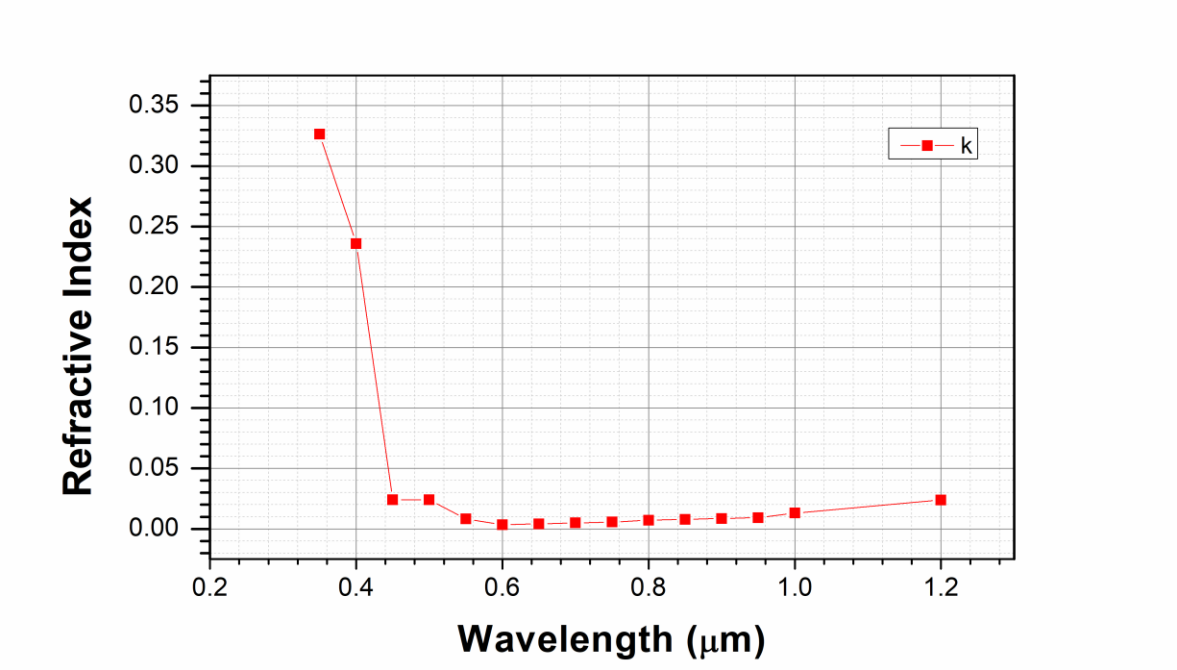

(e)

Figure 1.4 (a) Real and imaginary refractive index variation with wavelength of perovskite (b) Real and imaginary refractive index variation with wavelength of compact TiO_2 (c) Real and imaginary refractive index variation with wavelength of MoO_3 (d) Real and imaginary refractive index variation with wavelength of PCBM and (e) Imaginary refractive index variation with wavelength of Spiro MeOTAD

The data for the refractive index used in all the simulations for different materials is shown the figure 1.4 graphically.[21-24]

CHAPTER 2

Numerical simulation of PCBM and MoO_3 stacked electron and hole transport layer based perovskite solar cell

2.1Introduction

In the perovskite based solar PV cells, the need is to identify the best possible materials and their combinations for ETL and HTL. There are a number of inorganic metal oxides available as ETL like TiO_2 and their properties makes a strong case for their use but their availability is somewhat limited if we can reduce their amount to be used by adding another layer of an organic material such as PCBM then this can come up as a possible alternative. Similarly, if we can add a metal oxide like MoO_3 to the organic HTL like Spiro MeOTAD, the cost and ease of fabrication can be reduced and their application span can be increased. In this chapter, various materials and their combinations are used as ETL and HTL as a result of which EQE as high as 55% was reported and a PCE of over 14% was observed and in one of the devices, short circuit current density close to 18 $mAcm^{-3}$ was reported.

2.2Device Simulation and Methodology

Fig. 2.1(a) show the basic structure of perovskite solar cell used for simulation using Spiro MeOTAD as HTM of thickness 280nm and Compact TiO_2 as ETL of thickness 90nm and thickness of perovskite is 300nm . TCAD is used to create the structure, although the thickness of different regions have been varied in the subsequent structures, but it is done to obtain best possible results and for fair comparison.

In Fig. 2.1(b) PCBM of thickness 10nm has been added between compact TiO_2 and perovskite as ETM. In Fig. 2.1(c) a thin layer of MoO_3 of thickness 10nm and the thickness of PCBM is 10nm has been added after Spiro MeOTAD as HTM. In Fig. 2.1(d) MoO_3 of thickness 10nm has been added as HTL between Spiro MeOTAD and back contact, PCBM is removed. The electrodes, anode is made up of a high conductivity metal like Au with a work function of 5.1eV and cathode is transparent Fluorine doped Tin Oxide (FTO) with

work function of 4.4eV. The rest of the parameters are kept same. The length of all the structures is kept at 1000nm. The simulation is done considering basic recombination loses such as Shockley-Read-Hall (SRH), Auger and Radiative recombinations. The recombination constants used in this simulation are identical to as reported previously in chapter 1. The simulations performed are under AM 1.5 illuminations. All the structures proposed are two terminal devices simulated in TCAD Silvaco atlas software.

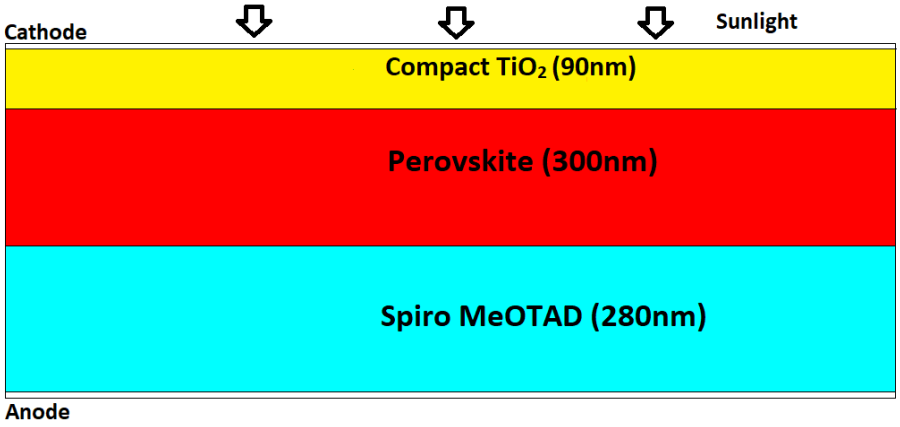

(a)

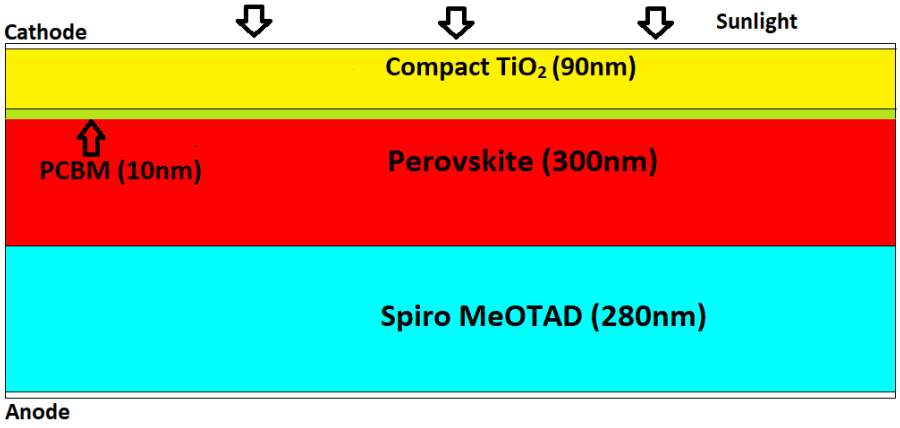

(b)

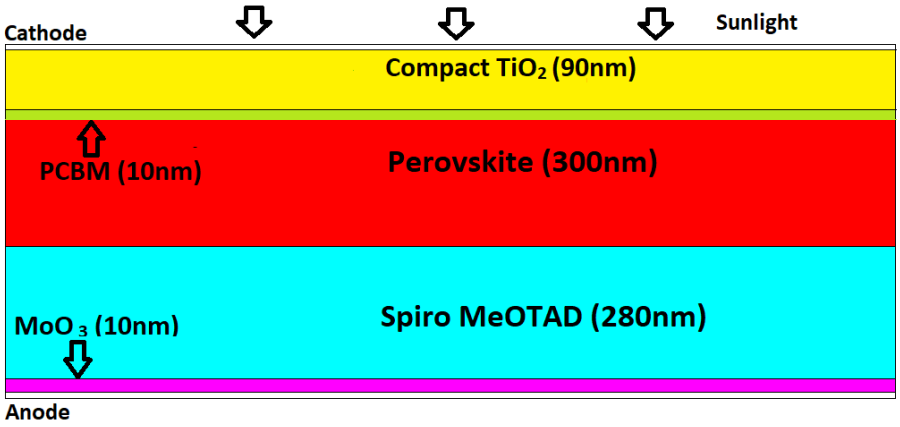

(c)

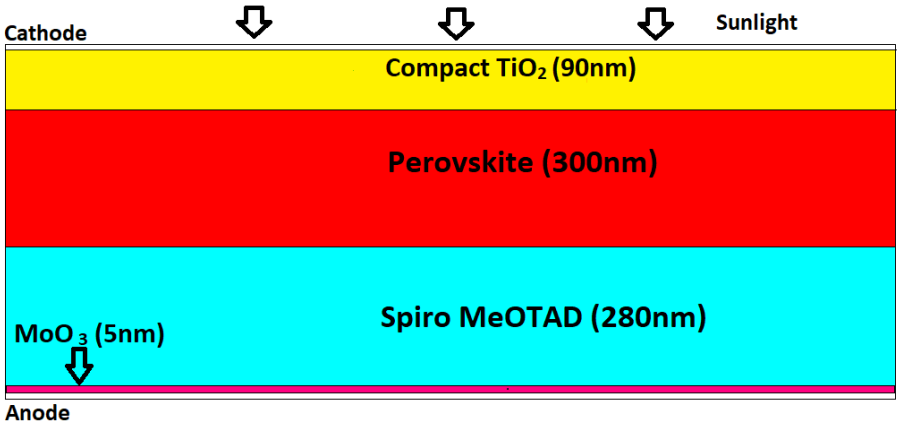

(d)

Figure 2.1 (a) Structure 1 i.e. basic structure with Compact TiO_2 as ETM and Spiro MeOTAD as HTM (b) Structure 2 with stacked PCBM layer between ETM and perovskite (c) Structure 3 with stacked PCBM layer between ETM and perovskite and stacked MoO3 layer between HTM and back contact and (d) Structure 4 with stacked MoO_3 between HTM and back contact, PCBM is removed.

2.3 Simulation Results and Discussion

Fig 2.2 compares the EQE of structures 1, 2, 3 and 4, all the curves obtained are from wavelength 350-700 nm. As evident from the curve, the peak from structures 2 and 3 is reached between wavelength 550-600 nm range while the peak for structures 1 and 4 is obtained at wavelength 430nm. The essential part is that the peak obtained from structures 2 and 3 have peaks at higher wavelength of 500-600 nm due to the addition of PCBM layer which affects 'blue' light that is the short wavelength light absorption which takes place at the surface of the perovskite whereas the green light is absorbed at the bulk of the perovskites' layer. This is because the EQE is affected due to the transmission losses in the solar cell with the addition of PCBM, the charge carriers have low collection probability due to high resistance or decreased mobility of electrons but high quantum energy is produced at low wavelengths and more electron hole pairs are generated as a result but as stated they are recombined at the HTL/ETL junctions.

Fig 2.3 compares J-V characteristics of the four structures in structures 2 and 3 at low anode current density of the order of is 0-0.5 $mAcm^{-2}$ and for the structures 1 and 4, the anode current density is $5mAcm^{-2}$ and goes upto 25 $mAcm^{-2}$ but the anode voltage for all the structures is about 1 V at zero Jsc as the carrier concentration and lifetime for structures 2 and 3 is low due to extra addition of PCBM and MoO_3. The anode current density is reduced as the collection probability decreases due to high resistance offered by the PCBM layer which affects the FF which in turn reduces the Jsc at low Voc .

Fig.2.4 (a) gives the variation of PCE of all the four structures. The losses are high in the 2^{nd} and 3^{rd} structures due to resistance of the PCBM layer causing a hindrance for the flow of electron which decreases its FF causing a decrease in PCE in comparison to structures 1 and 4. Moreover, it shows that the addition of MoO_3 has not affected the efficiency of the solar cell owing to its small thickness and comparable bandgap with Compact TiO_2. There is approximately 10% decrease in the PCE due to the addition of PCBM from structure1 to 2 because of the low conduction and valence band density which causes low input power in the perovskite region.

Fig 2.4 (b) shows the variation of FF for the structures even when the maximum current for structure 2 and 3 is low. The fill factor is still comparable and only a decrease of 13% is

observed between the lowest in structure 3 to the highest in structure 1. This is due to the fact that the maximum values for the current and voltage are comparable which is a consequence of relatively similar carrier lifetime in the perovskite layer in all the four structures.

Fig. 2.4 (c) shows Jsc variation in all the structures, because of the low optical losses and increased collection probability near the pero/PCBM interface of the small wavelength light aided by the small region of PCBM in structure 3 where the maximum short circuit current density Jsc is achieved. The low resistance path offered to the flow of electrons by PCBM also aids in high Jsc but only a small decrease of 2% is observed between the highest and lowest Jsc. The Jsc for structure 3 is lowest due to increased optical loses in the MoO_3.

Fig 2.4 (d) shows the difference between Voc of all the structures. Voc directly depends on mobility and carrier concentration and that's why it is highest for structure 4 followed by structures 1, 3 and 2. Only a marginal difference of 1.7% is observed between Voc of structure 1 and 3 chiefly due the low carrier concentration and mobility of PCBM.

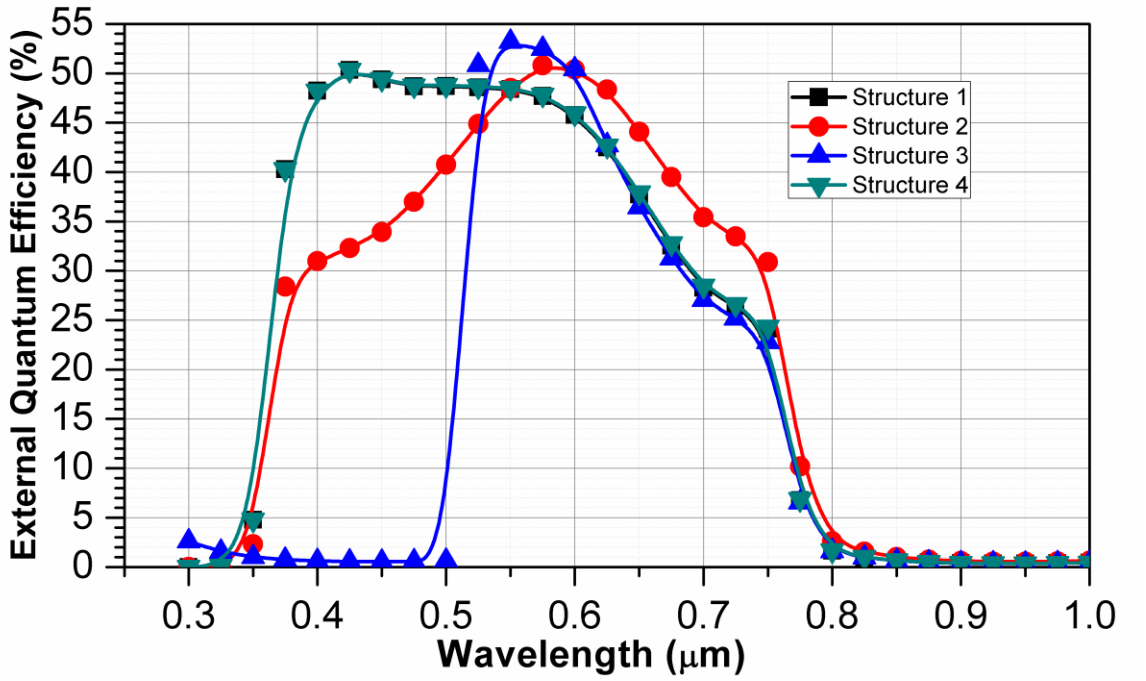

Fig. 2.2: Quantum Efficiency Curve (of structures 1, 2, 3 and 4).

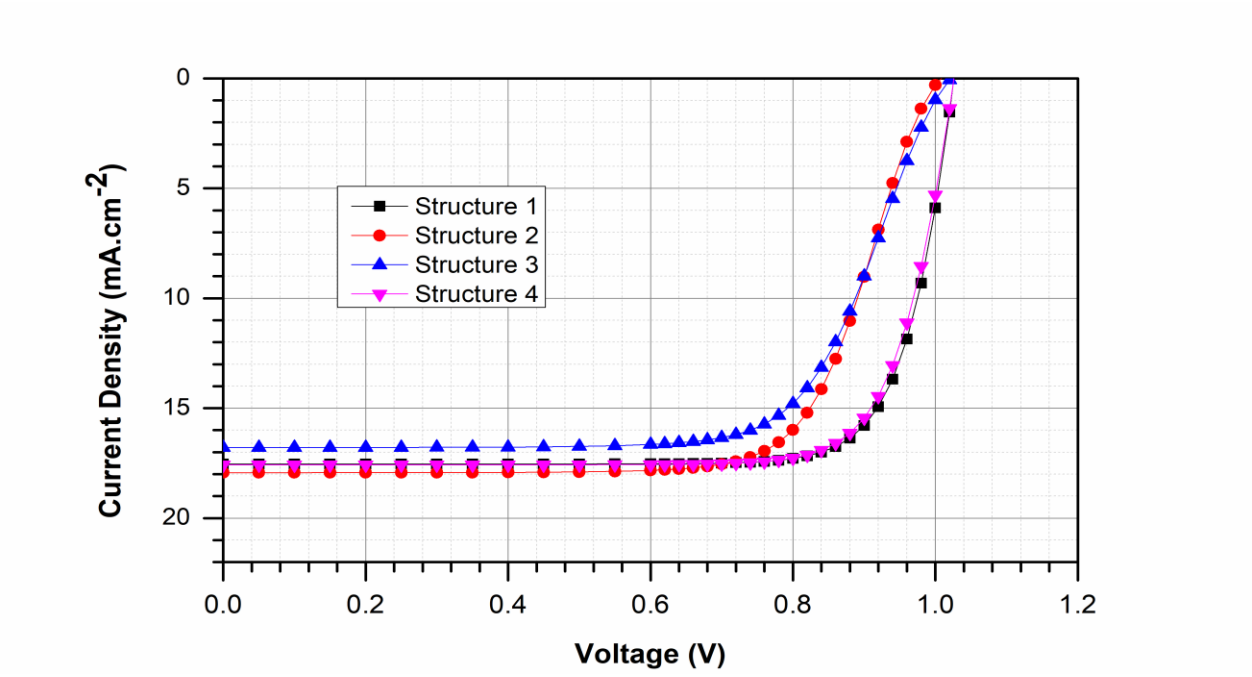

Fig. 2.3: J-V Characteristic Curve (of structures 1, 2, 3 and 4).

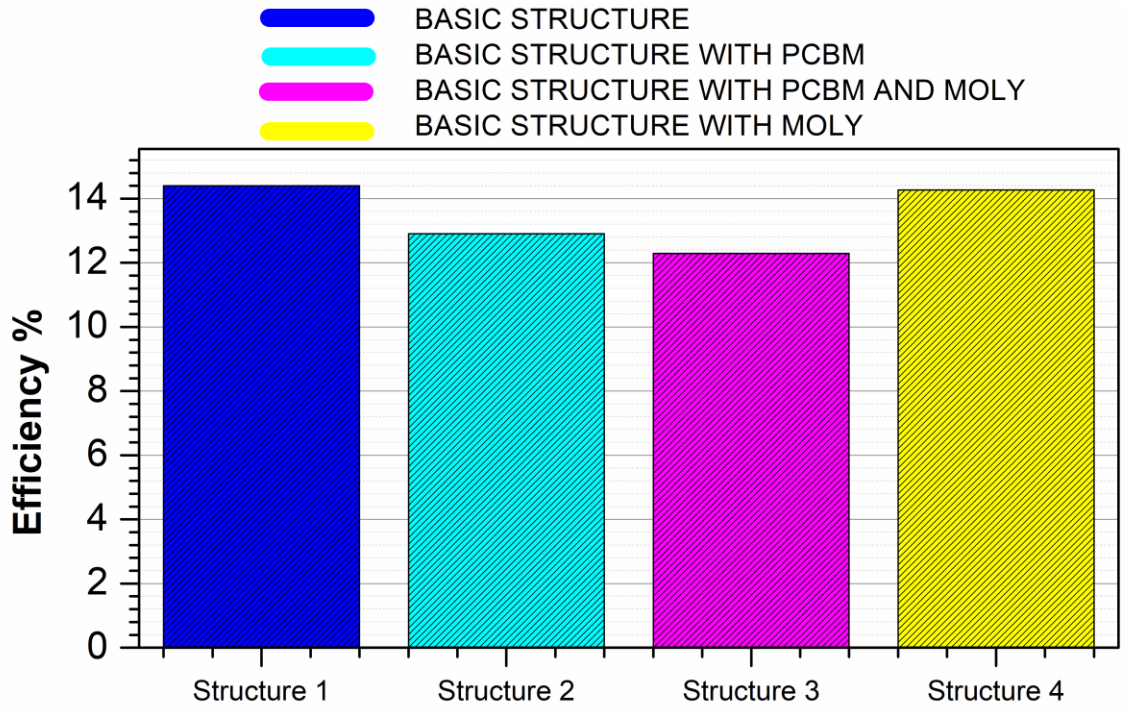

(a)

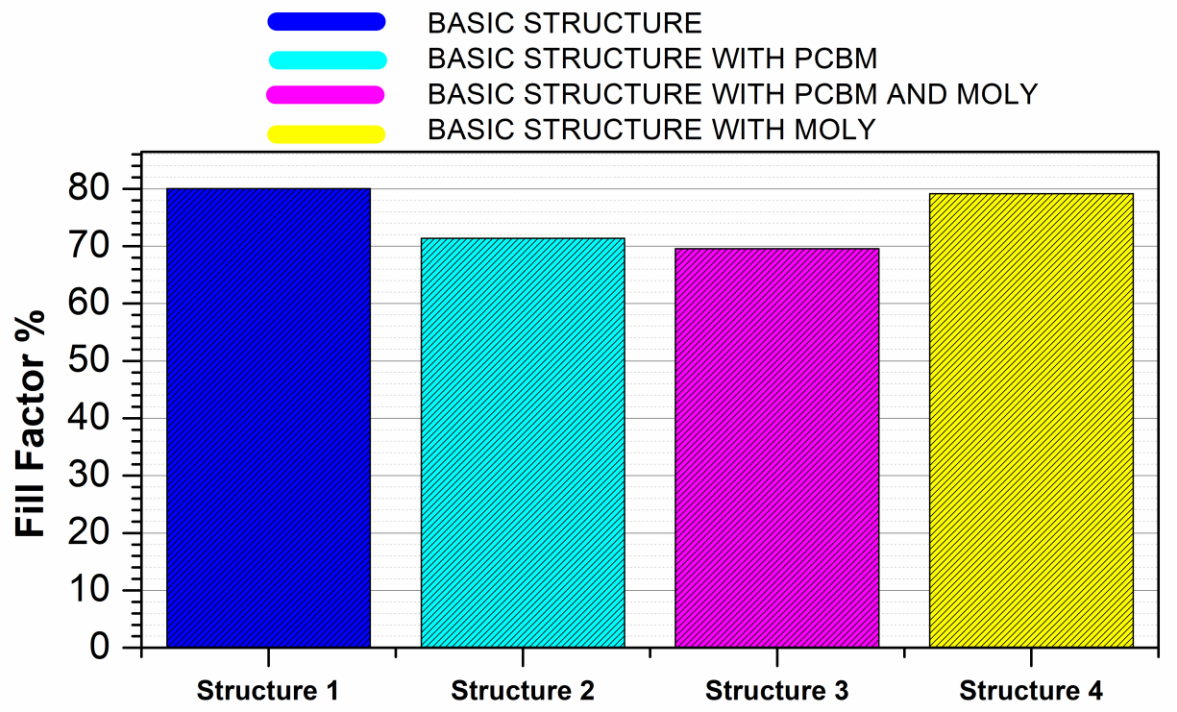
BASIC STRUCTURE
BASIC STRUCTURE WITH PCBM
BASIC STRUCTURE WITH PCBM AND MOLY
BASIC STRUCTURE WITH MOLY
Fill Factor %
0
10
20
30
40
50
60
70
80
Structure 1
Structure 2
Structure 3
Structure 4

(b)

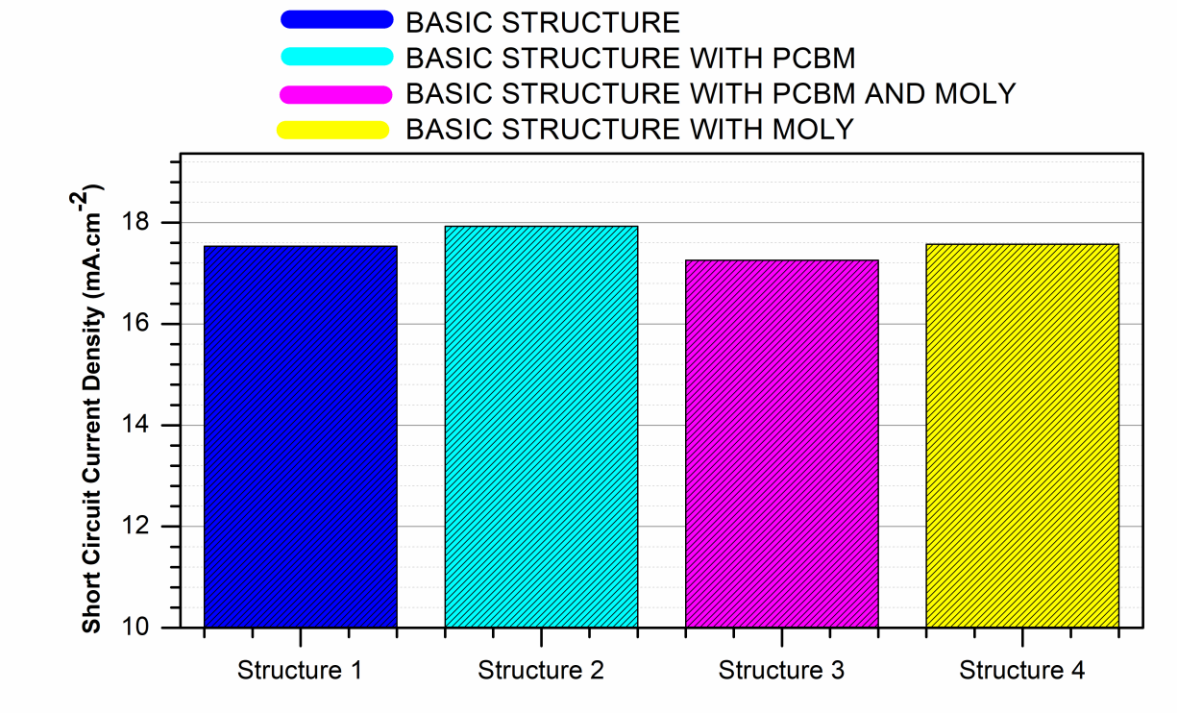
BASIC STRUCTURE
BASIC STRUCTURE WITH PCBM
BASIC STRUCTURE WITH PCBM AND MOLY
BASIC STRUCTURE WITH MOLY
Short Circuit Current Density (mA.cm-2)
10
12
14
16
18
Structure 1
Structure 2
Structure 3
Structure 4

(c)

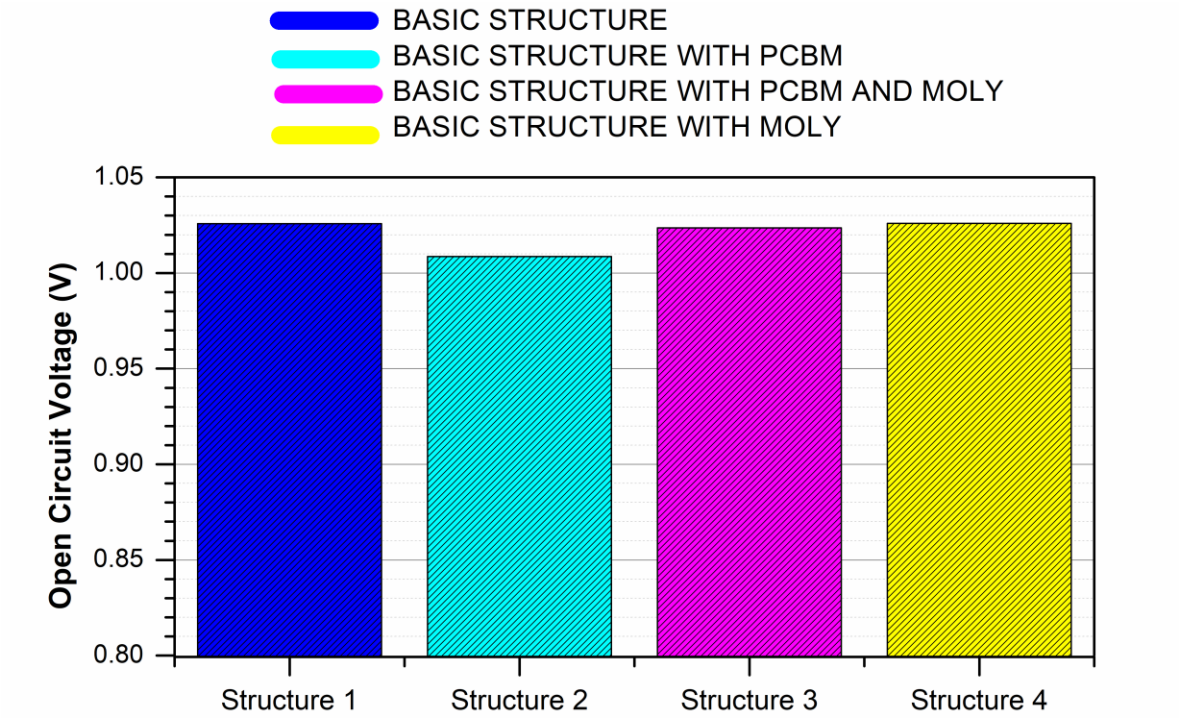

(d)

Fig. 2.4: (a) Power Conversion Efficiency (of structures 1, 2, 3 and 4) (b) Fill Factor (of structures 1, 2, 3 and 4) (c) Short Circuit Current Density (of structures 1, 2, 3 and 4) and. (d) Open Circuit Voltage (of structures 1, 2, 3 and 4).

2.4 Summary

In this work, the PV device was designed by using different material as HTL and ETL and combinations of these different materials was also simulated. The EQE, J-V curve, PCE, FF were obtained and analysed. In the first basic structure where compact TiO_2 was used as ETL and Spiro MeOTAD was used as HTL, modifications were made and PCBM and MoO_3 was used as ETL and HTL repectively. Although the large values of PCE, FF and V_{oc} far outweigh the disadvantage of low J_{sc} in first structure, there are certain applications of small portable electronic devices such as externally mounted energy sources where high J_{sc} of structure 2 and 3 can be useful. The EQE of Structure 4 clearly resembles the best possible outcome among the the four structures.It is our contention that the combinations of ETL and HTL should be decided depending on the usage. Overall the best results were obtained when back contact PCBM was removed and MoO_3 was employed as HTL in conjunction with Spiro MeOTAD.

CHAPTER 3

Optimization of molybdenum trioxide stacked HTL in perovskite based solar cell

3.1Introduction

In the conventional perovskite based solar cells, this chapter seeks to vary the thickness and doping of MoO_3 and compare the results so obtained. The reason for taking this approach is that the MoO_3 as HTL and its effects are yet to be fully understood and explored. Firstly in this chapter, the thickness of MoO_3 is varied from 5nm to 20 nm and it was observed that there is a drastic decrease in the short circuit current density by almost 60% as we increased the thickness. Further, when the doping was varied, the EQE went down from 55% for 10^{18} cm^{-3} carrier concentration to 50% for 10^{16} cm^{-3} carrier concentration. The cost of fabrication is reduced upon increasing the thickness and doping of deposition of MoO_3 and therefore this kind of exhaustive study becomes extremely crucial.

3.2 Device Structure and Simulation Methodology

Figure 3.1 (a) shows the layer of MoO_3 stacked between the anode and the spiro and is being used as an HTL. Here the width of MoO_3 is kept at 5nm, and perovskite thickness which is the active absorbent material is kept at 300 nm and the thickness of spiro is kept at 280 nm which is used as an HTL in conjugation with the MoO_3, compact TiO_2 is used as an ETL and its thickness is 90 nm. Only the thickness of MoO_3 is varied in the subsequent structures and the thickness of all the other layers are kept constant so that the results can be fairly compared. Although the small thickness of MoO_3 will pose some difficulties in fabrication but its advantages far outweigh those difficulties. The electrodes, anode is made up of a high conductivity metal like Au with a work function of 5.1eV and cathode is transparent Fluorine doped Tin Oxide (FTO) with work function of 4.4eV. The doping concentration of Compact TiO_2 is kept at $5x10^{19}$ cm^{-3} and that of PCBM is $1x10^{20}$ cm^{-3} they are both n type materials. The doping concentrations of perovskite, Spiro MeOTAD and MoO_3 are $2.14x10^{17}$ cm^{-3}, $3x10^{18}$ cm^{-3} and $1x10^{18}$ cm^{-3} respectively; they are all p type materials. In figure 3.1 (b) the thickness of MoO_3 has been increased to 10 nm and the rest

is kept same as the figure 3.1(a). In figure 3.1(a) structure 5, the doping of the MoO_3 is also varied from 10^{16} cm^{-3} to 10^{18} cm^{-3} to its effects. the SRH, radiative and auger recombination constants for MoO_3 are $10^{-9}cm^{-3}/s$, $10^{-14}cm^{-3}/s$ and 10^{-31} cm^{-3}/s respectively and carrier lifetime for MoO_3 is in the order of 10 nanoseconds as discussed in previous chapters. The length of all the structures is kept at 1000nm. The simulation is done considering basic recombination loses such as Shockley-Read-Hall (SRH), Auger and Radiative recombinations. The recombination constants used in this simulation are same as reported previously in chapter 1-table 1. The simulations performed are under AM 1.5 illuminations. All the structures proposed are two terminal devices simulated in TCAD Silvaco atlas software. The simulations performed are under AM 1.5 illuminations.

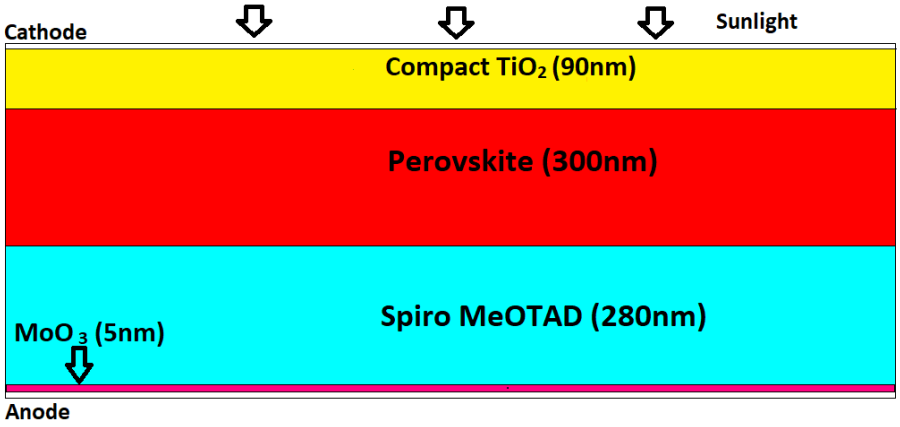

(a)

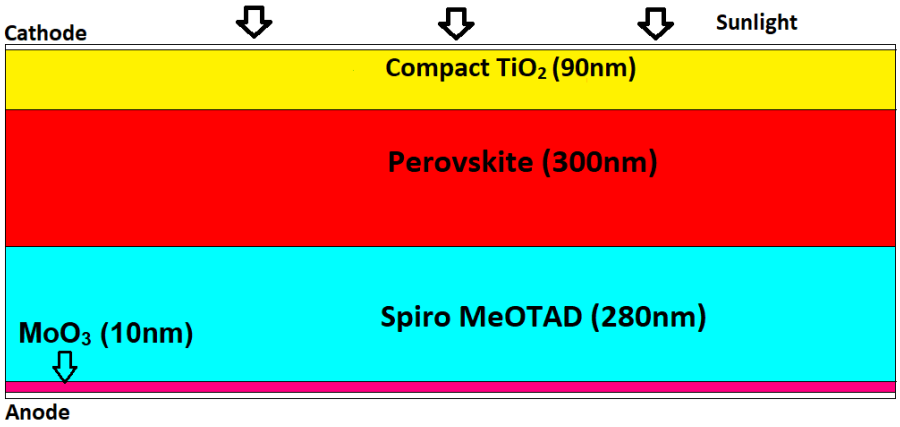

(b)

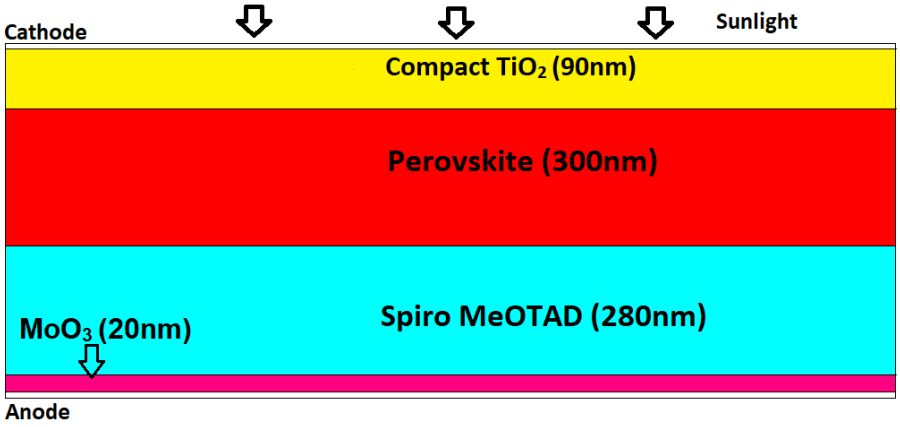

(c)

Figure 3.2 (a) Structure 5 with MoO_3 of thickness 5nm stacked between HTM and back contact (b) Structure 6 with increased thickness of 10 nm of MoO_3 stacked between HTM and back contact and (c) Structure 7 with stacked MoO3 layer of thickness 20nm between HTM and back contact.

3.3 Simulation Results and Discussion

In figure 3.2 (a), the PCE with the variation in the thickness of MoO_3 is shown. As we can see from the graph, the PCE is highest for the 5nm thickness and the difference of PCE between 10 nm and 20 nm thickness in almost negligible. This can be attributed to the fact the all the PCE above 10nm saturates in MoO_3 because the charge transportation for a thickness greater than 10nm is less as high resistance is offered to the path of travelling hole. The mobility of the MoO_3 is drastically decreased when the thickness is increased beyond 5 nm and therefore the number of charge carriers being collected at the anode starts decreasing which reduces the FF of the solar cell ultimately affecting the PCE. There is a gradual decrese in PCE as we decrease the thickness from 5 nm to 10 nm but once it reaches 10 nm, there is no decrease in PCE and it saturates. The 5 nm thickness yields the best results not only for PCE but also for FF and J-V curves. Decreasing the thickness below 5 nm is not considered suitable as it will pose numerous challenges during fabrication and different kinds of measures will be required to ensure that there is no contamination which will further add to the cost of fabrication.

Similarly in figure 3.2 (b), the fill factor between different thickness have been compared due to reason stated above and the 5 nm thickess structure yield the maximum FF. The FF is directly proportional to the PCE as discussed in chapter 1 so when the FF is decreased the PCE for the corresponding structure is affected accordingly. The FF is a measure of the useful energy or the light energy converted into electric energy so as evident from the figure 3.2 (b) the maximum useful energy is obtained from the structure having a thickness of 5 nm.

In figure 3.2 (c), the J-V curves for different thickness of MoO_3 are compared. The J-V curve for 20 nm thickness is essentially a straight line which is not useful in solar cell as the maximum power generated is very low which is due to the low J_{sc}. But the J-V curves for the 5 nm thickness and 10nm thickness are comparable. The interesting point is that even with low PCE and FF, the V_{oc} for 10 nm thickness is slightly higher than the 5 nm thickness and this is because V_{oc} depends on the saturation current I_o as discussed in chapter 1 eq (5) in the main absorbent layer of perovskite as less number of holes are being injected into the HTL due to its large thickness and the PV devices' internal electric field

increases which saturate the device much more quickly. This translated into a high V_{oc} for the 10 nm thickness as compared to the 5 nm thickness and as the thickness is increased, the PV device saturates at a faster rate and for the same reason, the PV device with 20 nm and 10 nm thickness of MoO_3 has comparable V_{oc}. The J_{sc} keeps on increasing as the thickness of the MoO_3 is decresed this is because the collection probability is increased i.e., more number of holes are collected for small thickness of MoO_3. The low J_{sc} here symbolizes high resistance of the PV device which inherently conveys the fact that less number of holes are successfully travelling through the HTL used here. There is a 60% decrease in the J_{sc} as we increased the thickness of MoO_3 from 5nm to 20 nm.

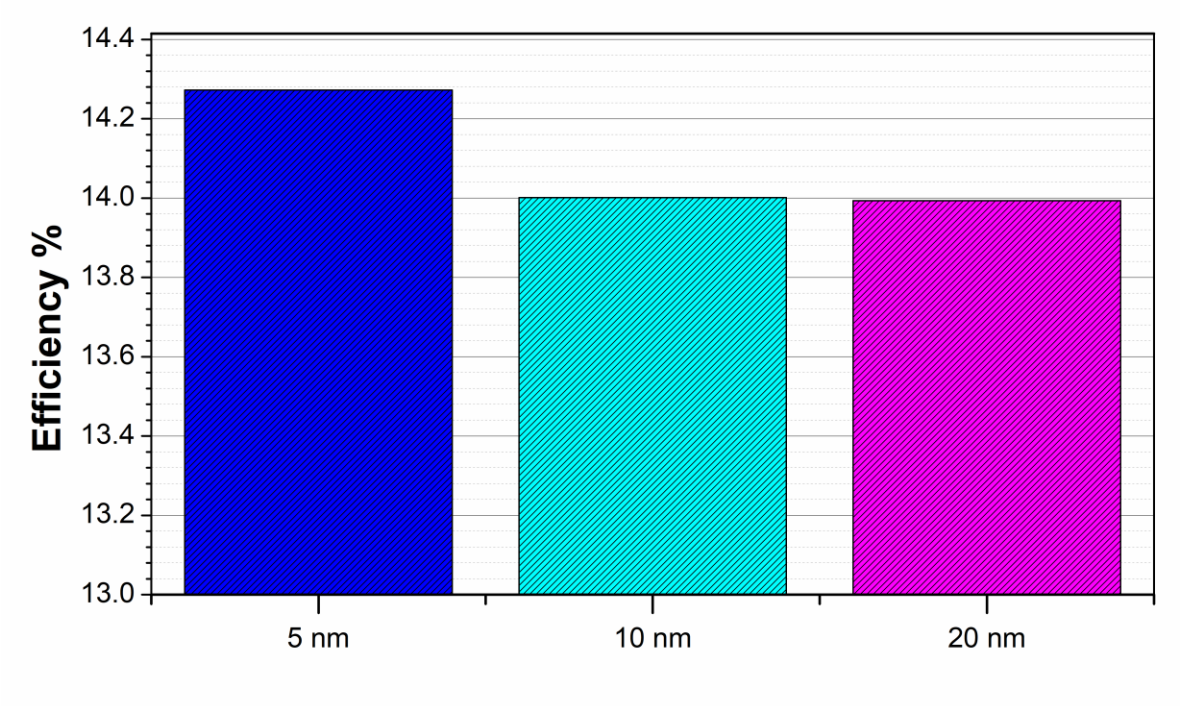

(a)

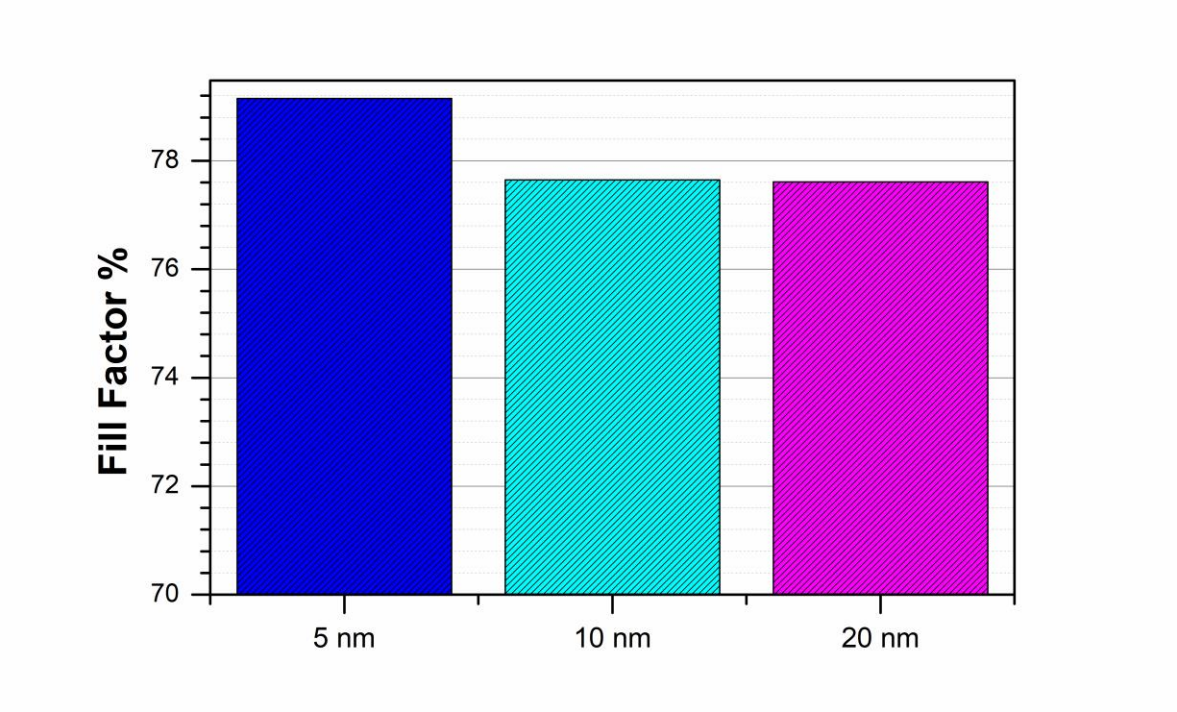

(b)

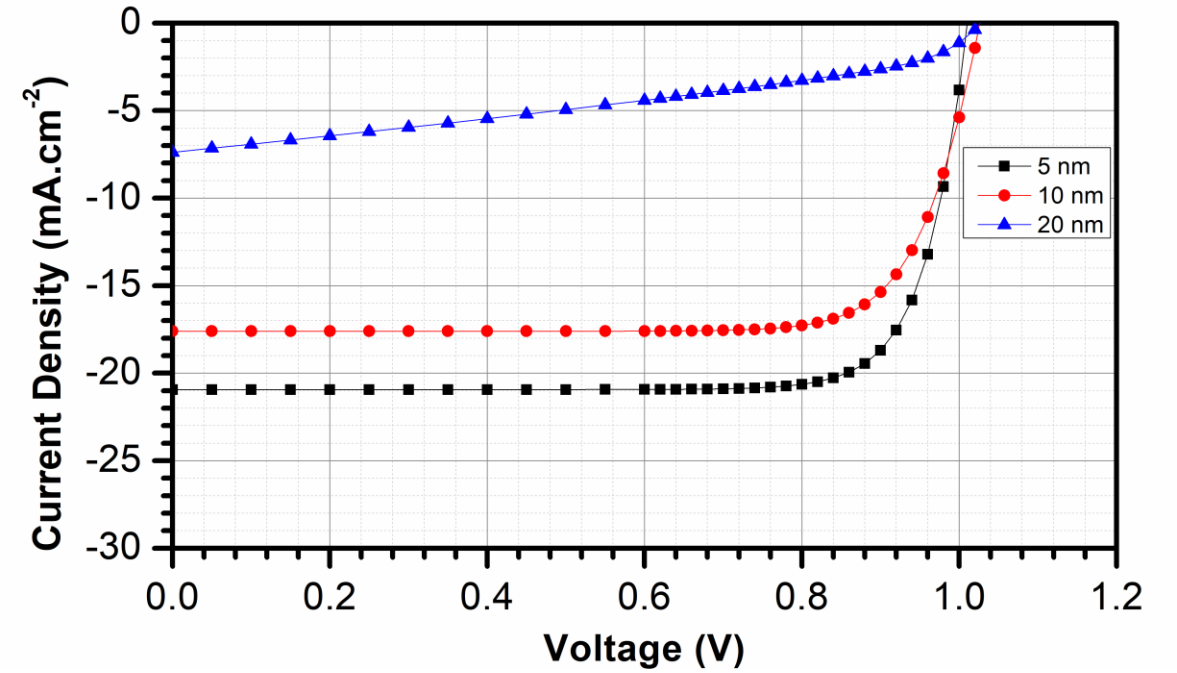

(c)

Figure 3.2 (a) Variation in Power Conversion Efficiency with varying thickness of MoO_3 in Structures' 1, 2 and 3 (b) Variation in Fill Factor with varying thickness of MoO_3 in Structures' 1, 2 and 3 (c) J-V curves with varying thickness of MoO_3 in Structures' 1, 2 and 3

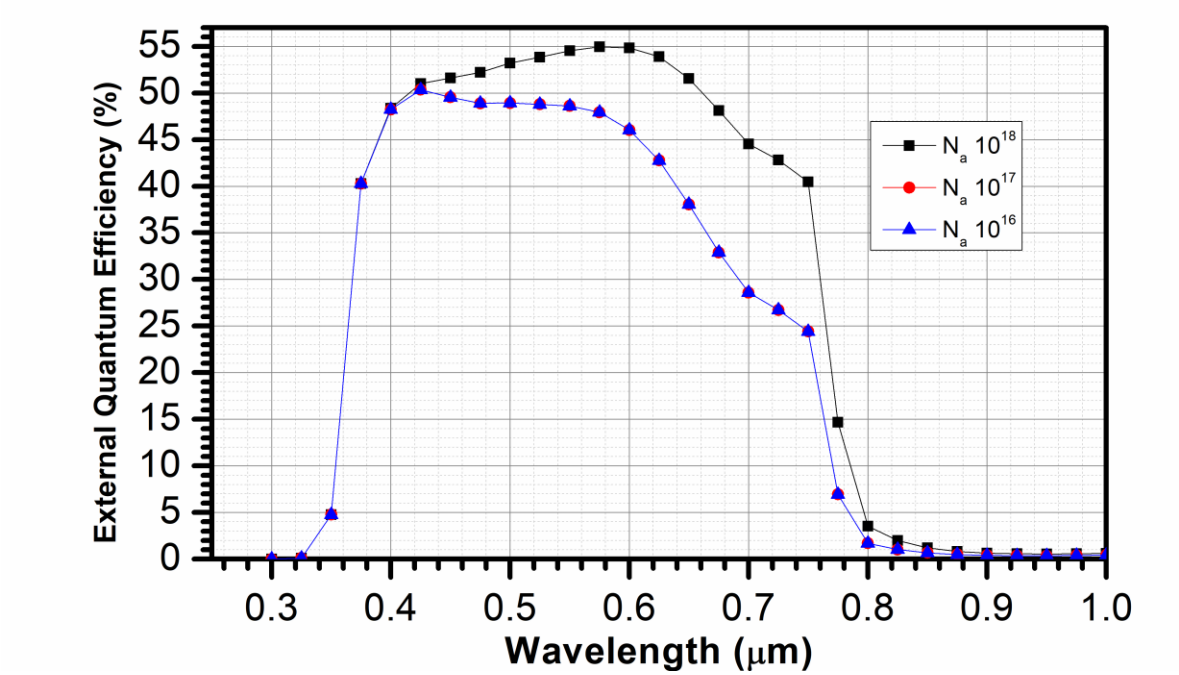

Figure 3.3 External Quantum Efficiency Curves with variation in doping of MoO_3

In figure 3.3, the variation in EQE is shown when the doping of MoO_3 is varied from 10^{18} to 10^{16} cm^{-3}. The EQE is a measure of the conversion rate from photons to the electron hole pairs generated. Addition of any kind of layer at the back end will affect the EQE at the red portion of spectrum i.e., the high wavelength light as this light has high penetration depth so it will be absorbed at the back end of the active layer or near the perovskite/HTL interface. The reason for the low EQE at low charge carrier concentration in MoO_3 is the decrease in mobility of MoO_3 which decreases the holes collected at the perovskite/HTL interface. Moreover, the low concentration MoO_3 achieves its highest peak of 50% in the blue region of spectrum as compared to the highly doped MoO_3 which enables the increased transportation of charge carriers due to high mobility so the charge carriers collected from the perovskite layer will receive a smooth passage through MoO_3 this leads to the EQE of as high as 55% which is not the case in lightly doped MoO_3. On further study, we found that the doping of all the HTL layers used should be equal and greater than the active absorbent layer by a factor of 10^2 cm^{-3} but less than by a factor of 10^4 cm^{-3} for the best possible results of EQE beacuse the mobilities of individual layers may vary but the flow of charge reamins same, so in order to facilitate a smooth charge carrier flow, doping should remain same. Further increasing the doping yielded no appreciable change in the

results as the least resistant path is already available. Increasing the doping adds to the cost of fabrication of semiconductors at nanoscale and may change the properties desired for its application in PV device. So it is considered wise to not increase or decrease the doping of the HTL layers too much and should be kept similar to active perovskite layer.

3.4 Summary

In this work, the PV device was designed by varying the width of the MoO_3 which is used here as an HTL in conjunction with Spiro MeOTAD. The width was varied from 5nm to 20 nm and variation in the PCE, FF and J-V curve were found. Although the large values of PCE, FF and J_{sc} far outweigh the the disadvantage of low V_{oc} in 5 nm thickness of MoO_3 as comapred to 10 or 20 nm thickness, there are certain applications of small portable electronic devices such as calculators where high V_{oc} can be useful. It is our contention that the thickness of the MoO_3 should be decided depending on the usage. Overall the best results were obtained for 5 nm thickness of MoO_3. Further the doping of the MoO_3 was varied and the EQE for the same was analyzed and it was concluded that the best rsults were obtained for a doping which is similar to the other material used as HTL and should be slightly greater than the dopingof the active layer. The ideal doping in our work was found to be 10^{18} cm^{-3}.

CHAPTER 4

CONCLUSION

4.1 Summary

We used perovskite as the primary absorbent layer or the active layer in all of the devices because of its attractive properties as discussed in chapter 1. Despite the fact that a good absorbent material with suitable bandgap is present yet the PCE is not increasing at a rapid rate as the materials used as HTL and ETL needs to be studied more thoroughly. In this study we covered the two main aspects associated with perovskite based PV cells

In the first chapter, different materials were used as ETL such as compact TiO_2 and PCBM, similarly different materials were used as HTL such as Spiro MeOTAD and MoO_3, combination of two or more of these materials were also employed in some of the simulations. From these analyses we concluded that the individual properties of materials do not govern the functioning and results of the PV cell but their combinations and their ability to act as desired by the absorbent material. The PCE is highest in the basic structure but at the expense of slight decrease in PCE higher Jsc and Voc can be obtained. For small current application structures 2 with stacked PCBM layer between ETM and perovskite and 3 with stacked PCBM layer between ETM and perovskite and stacked MoO_3 layer between HTM and back contact can be employed as it can generate same amount of voltage for small current these small solar cells can be used in electronic circuits. the sharp peak in the quantum efficiency curve at small wavelengths also supports the application span for structure 4 with stacked MoO_3 between HTM and back contact, PCBM is removed with large generation of electron hole pairs the theoretical efficiency of solar cells can easily be achieved.

In the second chapter, we discussed the simulation results by varying the thickness and doping of the MoO_3 layer which is used as an HTL and back contact PCBM was removed so that the thickness and the doping of the MoO_3 can be optimised. After studying the results it was concluded that the optimum thickness of the MoO_3 was found to be around 5nm at which the PV device yielded best results but we cannot completely rule out the thickness greater than 5 nm as it may find its application in low current devices as the V_{oc} is greater than that of PV device with MoO_3 thickness of 5 nm. The doping is found to be optimum at the higher side of 10^{18} cm^{-3} and in conjunction with the active layer and other materials used as HTL if

increasing the doping as it will add to the fabrication cost and yields not appreciable change in the result so it is advised to not increase the doping by too much either.

4.2 Future Prospects

- The low cost of fabrication of this device and attractive results makes it a prime candidate for its use in handheld electronic devices such as calculators, radios, televisions, LED lights and even cell phones. The proposed PV device can generate high power quickly and has maximum power greater than its counterparts therefore even with quick surges in power, they have a long life span which makes them ideal for their application in electronic devices.
- The generation of power at a large scale for the proposed device will require further study but so far the results are very promising. The aim is to use proposed device or its modification at Mega Watt scale power generation. The front contact of MoO_3 helps in increasing the PCE and in reducing the fabrication cost so that it can become economically feasible at industrial scale and easy installation is possible but it is still a long way from that. Our proposed device will help in realizing a PV cell which has all the aforementioned qualities.
- The proposed device will find its application in the automobile industry. The cars need sudden acceleration and deacceleration which comes about by varying the torque which is controlled by the current supplied by the source. The high J_{sc} supplied to the batteries used in the cars which are powered electrically by the proposed device can help solve that aspect of automobile industry if it can be mounted on an automobile as a secondary source.
- The silicon based solar powered street lights sometimes stop functioning when there are extreme weather conditions. So different manufacturing process is required for it to be used in different weather conditions like mountains, deserts, coasts etc. But no such problem was faced in our study and so the proposed device can be looked at as an alternative as only one manufacturing process will be required for the proposed device.

REFERENCES

[1] ITRPV, “ITRPV seventh edition version 2.pdf,” (2016).

[2] K. Yoshikawa, H. Kawasaki, W. Yoshida, T. Irie, K. Konishi, K. Nakano, T. Uto, D. Adachi, M. Kanematsu, H. Uzu and K. Yamamoto “Silicon heterojunction solar cell with interdigitated back contacts for a photoconversion efficiency over 26%” *Nature Energy*, Volume 2, Issue 5, pp. 17032, (2017) .

[3] P. Loper, B. Niesen, S. Moon, S. M. D. Nicolas, J. Holovsky, Z. Remes, M. Ledinsky, F. Haug, J. Yum, S. Wolf, C. Ballif, " Organic- inorganic halide perovskites: perspectives for silicon based tandem solar cells " *IEEE J. Photovoltaics* issue 4, 1545-1551, (2014)

[4] A. Richter, M. Hermie, S W. Glunz "Reassessment of the limitinf efficiency of the crystalline siliconsolar cells" *IEEE J. Photovoltaics* issue 3, 1184-1191, (2013)

[5] J. *Peña, M. A. Fierro, J. L. Konsak* “Chemical structures and performance of perovskite oxides". *Chemical Reviews 101 (7) 1981–2017.*

[6] S. De Wolf, K.Weinger. C.V. Koreaas “Organometallic halide perovskites: sharp optical absorption edge and its relation to photovoltaic performance,” *J. Phys. Chem. Lett.* 5, 1035–1039, (2014).

[7] M. A. Leguy, L. Beidret, L.A. Filoman, Z. Vienver “Reversible hydration of CH3NH3PbI3 in films, single crystals and solar cells” *Chem. Mater.* Issue 27, 3397–3407, (2015).

[8] N. G. Park, “Perovskite solar cells: an emerging photovoltaic technology,” *Mater. Today* 18(2), 65–72, (2015).

[9] G. E. Eperon et al., “Perovskite-perovskite tandem photovoltaics with optimized bandgaps,” *Science letters* 354(6314), 861–865 (2016).

[10] K. Mahmood, A. Saad Sarwarb, and M. Taqi Mehranb, " Current status of electron transport layers in perovskite solar cells: materials and properties"*Royal Society Of Chemistry*, 28, 17-03, (2017)

[11] Sandro Lattante “Electron and Hole Transport Layers: Their Use in Inverted Bulk Heterojunction Polymer Solar Cells” *Advanced Electronics*, 3, 132-164, (2014)

[11] Philipp L¨oper, Bjoern Niesen, Soo-Jin Moon, S´ılvia Mart´ın de Nicolas, Jakub Holovsky, Zdenek Remes, Martin Ledinsky, Franz-Josef Haug, Jun-Ho Yum, Stefaan De Wolf, and Christophe Ballif, "Organic–Inorganic Halide Perovskites:Perspectives for

Silicon-Based Tandem Solar Cells" *IEEE Journal of Photovoltaics,* vol4. number 6, 172-11, (2014)

[12] Y. Hayashi, H.takizawa, "Nanoparticle fabrication" *Reasearch gate,* pp109-120, 17-12 (2008)

[13] R. Pandey, R. Chaujar "Technology and computer aided design of 29.5% efficient perovskite/interdigitated baccontact silicon heterojunction mechanically stacked tandem solar cell for energy efficient apllications" *Journal of Photonics of Energy* 100, 656-666, (2016)

[14] L. Tzabari, N. Tessler "SRH recombination in P3HT:PCBM solar cells observed under ultralow light intensities" *Journal of Applied Physics* 109, 064501, (2011)

[15] F. Laquai, D. Andrienko, C. Deibel, D. Neher "Charge carrier generation, recombination and extraction in polymer fullerene bulk heterojunction organic solar cells" *Springer International Publishing Elementary process in Organic Photovoltaics* 23 (31), 3597-3602, (2011)

[16] J. You, C. Chen, Z. Hong, K. Yoshimura, K. Ohya, R. Xu, S. Ye, J. Gao, G. Li, Y. Yang "10.2% power conversion efficiency polymer tandem solar cells consisting of two identical sub cells" *Advanced Materials* 25 (29), 3973-3978, (2013)

[17] W.H. Lee, S. Chuang, H. Chen, W. Su, C Lin "Exploiting optical properties of P3HT:PCBM films for organic solar cells with semitransparent anode"*Thin Solid Films* 518 (24), 7450-7454, (2010)

[18] F. Monestier, J. Simon, P. Torichio, L. Escoubas, F.Flory, S. Bailey, R. Bettignies, S. Guilerez, C. Defranoux "Modelling the short circuit current density of polymer solar cells based on P3HT:PCBM blend "*Solar Energy Materials and Solar Cells* 91(5), 405-410, (2007)

[19] S. Kirschner, N. Smith, K. Wepasnick, H. Katz, B. Kirby, J. Borchers, D. Reich " X-Ray and neutron reflectivity and electronic properties of PCBM poly Styrene blends and bilayers" *Journal of Material Chemistry* 22 (10), 4363-4370, (2012)

[20] M. W. Alama, Z. Wanga, S. Nakaa and H. Okadaa "Temperature Dependence of Barrier Height and Performance Enhancement of Pentacene Based Organic Thin Film Transistor with Bi-Layer MoO3/Au Electrodes" *Current Nanoscience* , 9, 407-410, (2013) .

[21] Laurie J. Phillips, Atef M. Rashed, Robert E. Treharne, James Kay, Peter Yates, Ivona Z. Mitrovic, Ayendra Weerakkody, Steve Hall, Ken Durose “Dispersion relation data for methylammonium lead triiodide perovskite deposited on a (100) silicon wafer using a

two-step vapour-phase reaction process" *Science Direct* Volume 5, December , 926-928, (2015).

[22] C. Stelling, C. R. Singh, M. Karg, T. A. F. König, M. Thelakkat, "M. Retsch. Plasmonic nanomeshes:their ambivalent role as transparent electrodes in organic solar cells", *Science. Reports.* 7, 42530, (2017) .

[23] M. Vos, B. Macco, N. F. W. Thissen, A. A. Bol, W. M. M. Kessels, "Atomic layer deposition of molybdenum oxide from $(N^tBu)_2(NMe_2)_2Mo$ and O_2 plasma", *Journal Vac. Scientific Technology A* 34, 01A103, (2016).

[24] T. Siefke, S. Kroker, K. Pfeiffer, O. Puffky, K. Dietrich, D. Franta, I. Ohlídal, A. Szeghalmi, E.-B. Kley, A. Tünnermann, "Materials pushing the application limits of wire grid polarizers further into the deep ultraviolet spectral range" *Advance. Opical. Mater.* 4, 1780–1786, (2016).